

## Influence of DEF expansion on mechanical behavior under uniaxial compressive stress evaluated by Digital Image Correlation

Misato Fujishima <sup>(1)</sup>, Taito Miura <sup>(2)</sup>, Yuichiro Kawabata <sup>(3)</sup>, Hikaru Nakamura <sup>(4)</sup>

(1) Department of Civil Engineering, Nagoya University, Nagoya, Japan, [fujishima.misato@i.mbox.nagoya-u.ac.jp](mailto:fujishima.misato@i.mbox.nagoya-u.ac.jp)

(2) Department of Civil Engineering, Nagoya University, Nagoya, Japan, [t.miura@civil.nagoya-u.ac.jp](mailto:t.miura@civil.nagoya-u.ac.jp)

(3) Port and Airport Research Institute, Yokosuka, Japan, [kawabata-y@p.mpat.go.jp](mailto:kawabata-y@p.mpat.go.jp)

(4) Department of Civil Engineering, Nagoya University, Nagoya, Japan, [hikaru@cc.nagoya-u.ac.jp](mailto:hikaru@cc.nagoya-u.ac.jp)

### Abstract

*Delayed ettringite formation (DEF) is a deterioration phenomenon by which the expansion of cement paste causes internal cracks in the concrete. Previous experimental data on the relationship between the expansion and compressive behaviors were obtained from the stress-free concrete. On the contrary, it is not yet clear whether this relationship can be directly applied to the restraint condition, because the internal crack pattern due to DEF-induced expansion indicates a directionality due to the anisotropy of expansion under a restraint stress. In this study, as a fundamental investigation for assessing the relationship between internal crack and the mechanical behavior, the reduction in compressive properties due to DEF-induced expansion under the stress-free condition is experimentally evaluated by considering the internal crack distribution. In this experiment, uniaxial compression tests with two types of compressive loading, namely monotonic and stepwise cyclic loading, are applied to cylindrical concrete specimens with 0.0, 0.1, 0.5, 1.3, and 2.0 % DEF-induced expansion levels under the stress-free condition. In monotonic loading, digital image correlation (DIC) is applied during compressive loading to visualize the distributions of compressive and tensile principal strains. In stepwise cyclic loading, elastic and plastic strains during cyclic loading at a certain stress level are identified. The results indicate that the compressive strength and elastic modulus reduced with the expansion. The result of DIC at a small expansion of 0.1 % indicates the existence of debonding cracks at the paste-aggregate interface even at a low stress level. At 0.5 % expansion and above, debonding cracks exist at all paste-aggregate interfaces and cracks also propagated to the mortar. In the case of stepwise loading, the plastic strains significantly increase with the expansion, while the elastic strains at the compressive strength reach approximately 1200 microstrains in all expansion levels.*

**Keywords:** compressive behavior, delayed ettringite formation, digital image correlation, internal crack, loading type

## 1. INTRODUCTION

Delayed ettringite formation (DEF) is a deterioration phenomenon by which the cement paste expands, causing internal cracks to be formed in the concrete [1,2]. The stress-free expansion due to DEF often reaches up to 2 % and even more, which is considerably larger than alkali-silica reaction (ASR)-induced expansion. Internal cracks caused by DEF-induced expansion have a unique tendency to generate debonding cracks at the paste-aggregate interface. Many researchers have experimentally observed that the reduction in the mechanical properties of concrete due to DEF is larger than that due to ASR; specifically, the elastic modulus drastically decreases at the initial expansion [3-6].

Both ASR and DEF induce the characteristic expansion behavior under restraint conditions. In the case of ASR, the expansion in the direction perpendicular to the restraint stress is larger than that under the stress-free condition [7,8]; this phenomenon is called expansion transfer, which could not be experimentally observed by other researchers [9]. Hence, the anisotropy of ASR-induced expansion under the restraint condition is still controversial. By contrast, in case of DEF, the volumetric expansion under uniaxial restraint stress decreases (by approximately 20 % according to [4,10]) corresponding to expansion in the direction perpendicular to the restraint stress less than that under the stress-free condition. Recently, the change in compressive properties due to the directionality of internal cracks was reported [11]. In that study, prism specimens extracted from existing slabs deteriorated by ASR

exhibited two types of internal crack patterns (horizontal and vertical) and the compressive properties of specimens were determined. The results revealed that the compressive strength and stiffness are larger for specimens with vertical cracks than for those with horizontal cracks. These results indicate that the compressive property change is affected by the directionality of internal cracks. It is possible that internal cracks due to DEF-induced expansion also follow the same trend. Therefore, it is important to understand the causal correlation between the anisotropy of expansion and the internal crack pattern because internal cracks due to the expansion under the restraint condition have a directionality. While the relationship between the generation and propagation of DEF-induced internal cracks under the stress-free condition and the reduction in the mechanical property has been reported [5, 12-18], the effect of directionality of internal cracks formed due to the expansion under the restraint condition on the mechanical behavior remains to be investigated.

Previously, the relationship between expansion due to DEF and the reduction in compressive properties has been investigated. However, internal cracks possibly indicate directionality due to the expansion under the restraint condition; for example, massive concrete is always affected by self-weight, which makes it difficult to predict the deformation performance by directly applying the relationship between the expansion and the reduction in mechanical properties. Therefore, it is necessary to investigate the reduction mechanism of compressive properties based on internal crack patterns instead of the expansion. In this study, the relationship between internal cracks due to the expansion under stress-free condition and the mechanical behavior was focused as a fundamental investigation. In particular, uniaxial compressive loading was applied to concrete specimens deteriorated by DEF under the stress-free condition to precisely understand the change in compressive properties due to DEF using digital image correlation (DIC). Furthermore, the development of plastic and elastic strain was clarified by stepwise cyclic loading. From the experiment results, the mechanical response of internal cracks under compressive stress was discussed.

## 2. EXPERIMENTAL OVERVIEW

In this experiment, cylindrical concrete specimens deteriorated by DEF under the stress-free condition were used, and two types of uniaxial compressive loading (monotonic loading and stepwise cyclic loading) were applied to the specimens. By applying monotonic loading, the reduction in the compressive strength and elastic modulus with increasing expansion was determined. In addition, under monotonic loading, DIC was used to visualize the distribution of compressive and tensile principal strains on the region of interest (ROI). In the stepwise cyclic loading, the cyclic loading was carried out until plastic deformation possibly occurred at a certain stress level, and the effect of the plastic deformation on compressive properties was investigated. In addition, the development of plastic and elastic strains with increasing stress levels was clarified to assess the mechanical response of internal cracks under compressive stress.

### 2.1 Specimens

First, cylindrical specimens of dimensions  $\Phi 100$  mm  $\times$  200 mm and based on the mix proportion shown in Table 2.1 were prepared.  $K_2SO_4$  was added as an admixture to accelerate DEF-induced expansion. The water-to-cement ratio (including  $K_2SO_4$ ) was 0.49. The specimens were placed in a high-temperature oven 4 h after casting, heated from 20°C to 90°C at a rate of +46.7°C/h for 1.5 h, cured at 90°C for 12 h, and cooled to 20°C at a rate of -7°C/h for 10 h. After the specimens were demolded, they were wrapped with plastic film and cured at 20°C for 28 days. After curing, they were immersed in water and the expansion test was started. When the expansion reached 0.1, 0.5, 1.3, and 2.0 %, the specimens were taken out from water and exposed to air for one or two days to stabilize the water inside the concrete before conducting the loading tests. This is because the compressive strength changes due to the water content inside the concrete [19]. To measure the expansion, the change in the length of the specimen was measured using studs positioned on the specimen as shown in Figure 2.1. The length change measurements of six specimens were obtained. The longitudinal expansion was obtained by dividing the longitudinal length change measured at two sides of the specimens by the initial length.

For monotonic loading, monotonic loading with DIC, and stepwise cyclic loading, two specimens each were used in all expansion level cases except for control specimens. For such control specimens, two specimens were subjected to monotonic loading and one specimen to cyclic loading; DIC and stepwise cyclic loading were not carried out.

Table 2.1: Mixture proportion of the concrete

Unit content (kg/m <sup>3</sup> )				
W	C	S	G	K <sub>2</sub> SO <sub>4</sub>
173	337	798	965	18.85

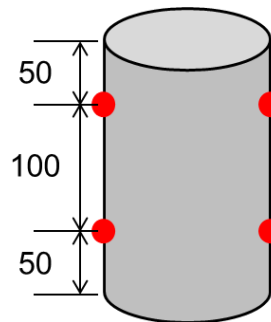


Figure 2.1: Measurement points on the specimens

## 2.2 Loading conditions

### 2.2.1 Monotonic loading

The uniaxial compression loading tests were performed using a high-stiffness universal testing machine. The aim of the experiment was to assess the effect of internal cracks formed due to DEF-induced expansion on the mechanical properties; therefore, the friction between the loading jigs and the specimen was removed. This was achieved by placing on the top and bottom of the specimen two Teflon sheets (0.05 mm thick) with silicone grease inserted between them. Four LVDTs were placed around the specimen to determine the displacement between the loading and supporting plates; this displacement is almost the same as the length change of the whole specimen in the longitudinal direction. The strain in the longitudinal direction was defined as the average of four displacement values divided by the length before loading. The loading rate was approximately 0.3 kN/s. After the compressive strength was reached, cyclic loading was applied to the specimens to obtain its overall post-peak behavior to avoid a brittle failure. However, control specimens and 0.1 % expansion of the specimens indicated brittle failure, because of which the post-peak behavior could not be determined.

### 2.2.2 Stepwise cyclic loading

The stress–strain relationship during stepwise cyclic loading of the specimens is shown in Figure 2.2. Through this type of loading, the mechanical response of internal cracks to plastic deformation was assessed at various stress levels in the pre-peak stage. In the stepwise cyclic loading, cyclic loading at a certain stress level was carried out as long as plastic strain developed. When the plastic strain was not progressing anymore, the cyclic loading was stopped and the next stress level was applied. In terms of cyclic loading, the stress levels of 25, 50, and 75 % were applied but those of 50, 75 % were applied for specimens having reached 0.5 % expansion level and 50 % for those that reached 2.0 % expansion level. The reloading stress was approximately 2.5 MPa for 0.5 % expansion and less, and 0.6 MPa for 1.3 and 2.0 % expansion levels. Other loading conditions were the same as those in monotonic loading.

The definition of elastic and plastic strains in this experiment is shown in Figure 2.2. First, the point where the maximum strain was achieved after unloading and the starting point of reloading were connected; then, the intersection of the connecting line and the x-axis was obtained. The x-coordinate of the intersection was defined as the plastic strain, and the difference between the maximum strain and the plastic strain was defined as the elastic strain. These strains were calculated in all cycles.

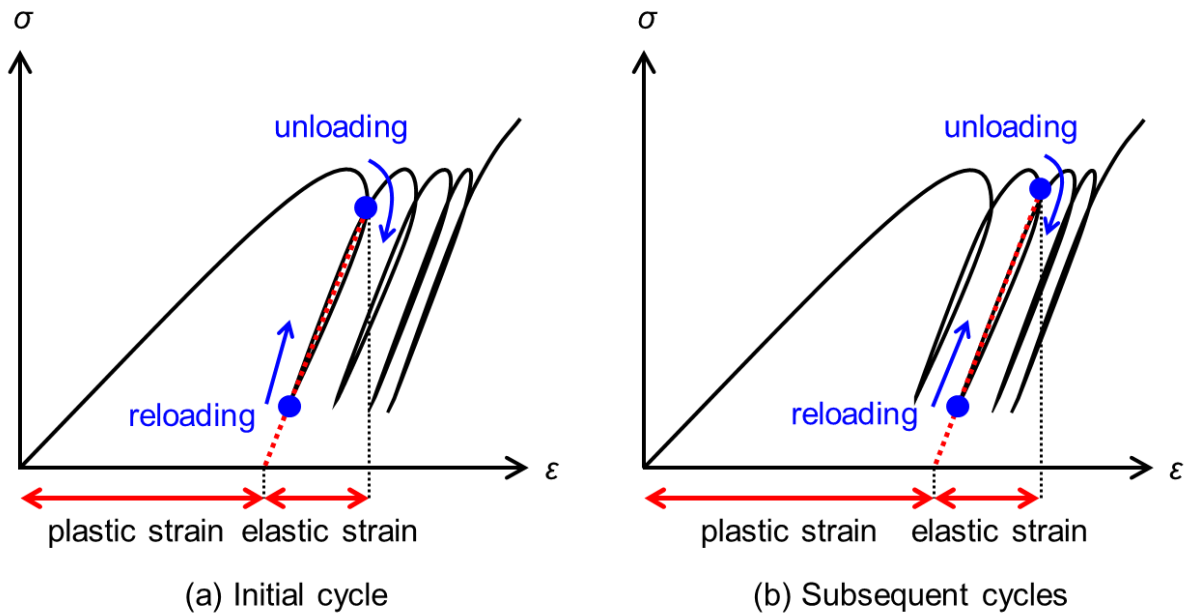


Figure 2.2: Definition of plastic and elastic strain

### 2.3 Digital Image Correlation (DIC)

To observe the internal cracks formed at the cross-sectional area of the cylindrical specimens, the specimens were cut and DIC was performed during monotonic loading to obtain the strain distribution in this ROI. The setup of the monotonic loading test with DIC is shown in Figure 2.3. The cylindrical specimens were cut at 50 mm from the central axis, and red and black points were sprayed on the ROI. A black curtain was placed in the background of the specimen, and the cross-sectional area, which is the ROI, was illuminated using two LED lights placed in front of the specimen. Further, the ROI was photographed every 2 seconds during compressive loading using a digital camera (Nikon D5500). The other loading conditions were the same as those in monotonic loading. DIC processing was performed on the resulting image data using the software GOM Correlate supported by GOM.

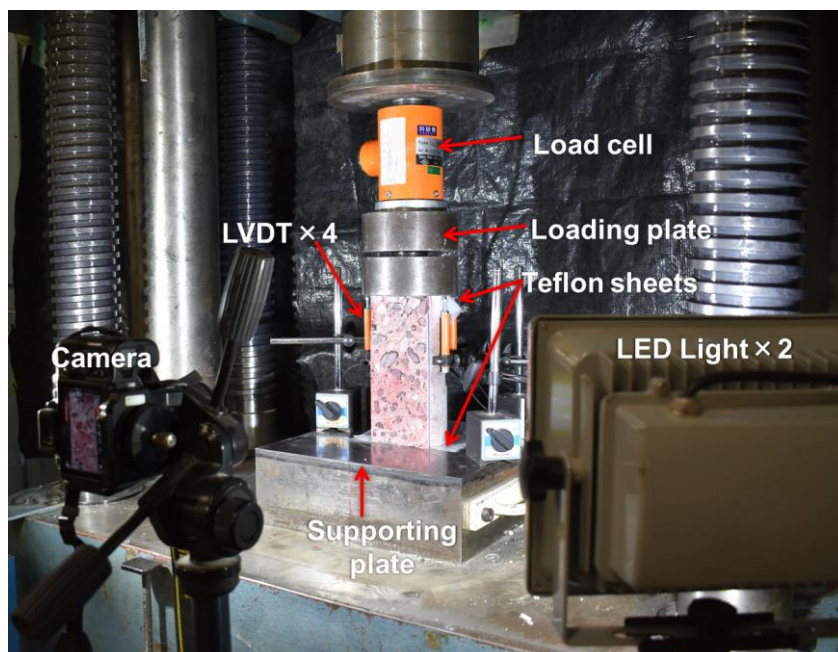


Figure 2.3: Experimental setup for compression tests with DIC

### 3. EXPERIMENTAL RESULTS

#### 3.1 Expansion

Figure 3.1 shows the evolution of expansion in the specimens. In this figure, the average expansion of the 6 specimens is shown and the error bars indicate the minimum and the maximum expansion. The expansion increased after 50 days and then significantly evolved until 125 days before reaching a plateau at approximately 2.0 %. The compressive properties of the specimens were measured at 0.1, 0.5, 1.3, and 2.0 % expansion levels, indicated by the red points in Figure 3.1.

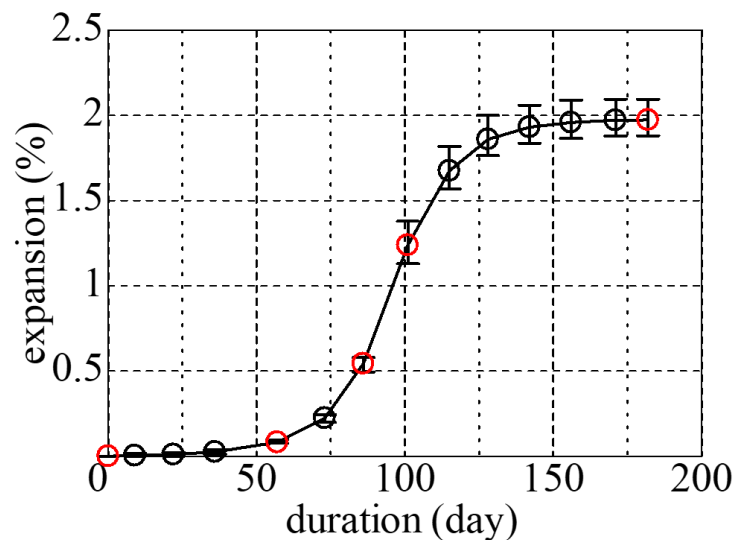


Figure 3.1: Longitudinal expansion of concrete

#### 3.2 Change in compressive behaviors

The relationships between the compressive strength and elastic modulus and the expansion of the specimens are shown in Figures 3.2 (a) and (b), respectively. The results of all compressive loading patterns are indicated in the figure, but the elastic modulus was not determined in the case of stepwise cyclic loading. The results show that the compressive strength linearly decreased until 0.5% expansion, then further decreased until 1.3 % expansion at a lower rate, and finally decreased down to reach a plateau at a ratio of about 13.3%. The elastic modulus largely reduced from the beginning of expansion, but with a trend significantly different from that of the compressive strength. The elastic modulus further reduced at 0.5 % expansion, then decreased at a slower rate, and finally decreased down to a ratio of 5.4 %. In this experiment, the reduction in elastic modulus was larger than that in compressive strength. Beyond the 1.3 % expansion, the compressive strength and elastic modulus did not change largely. In addition, it was found that the loading type did not affect the compressive properties.

Normalizing the compressive strength and the elastic modulus with control cases, the results of this experiment were compared with the previous experimental results [5,12-17], as shown in Figures 3.2 (c) and (d). This indicates that the reduction in compressive properties in this experiment was larger than that in the previous experiments. In this study, the friction between the loading and supporting plates and the specimen was reduced in order to understand the relationship between the internal crack due to DEF-induced expansion and the reduction in compressive properties, which may be different from the case of the previous studies.

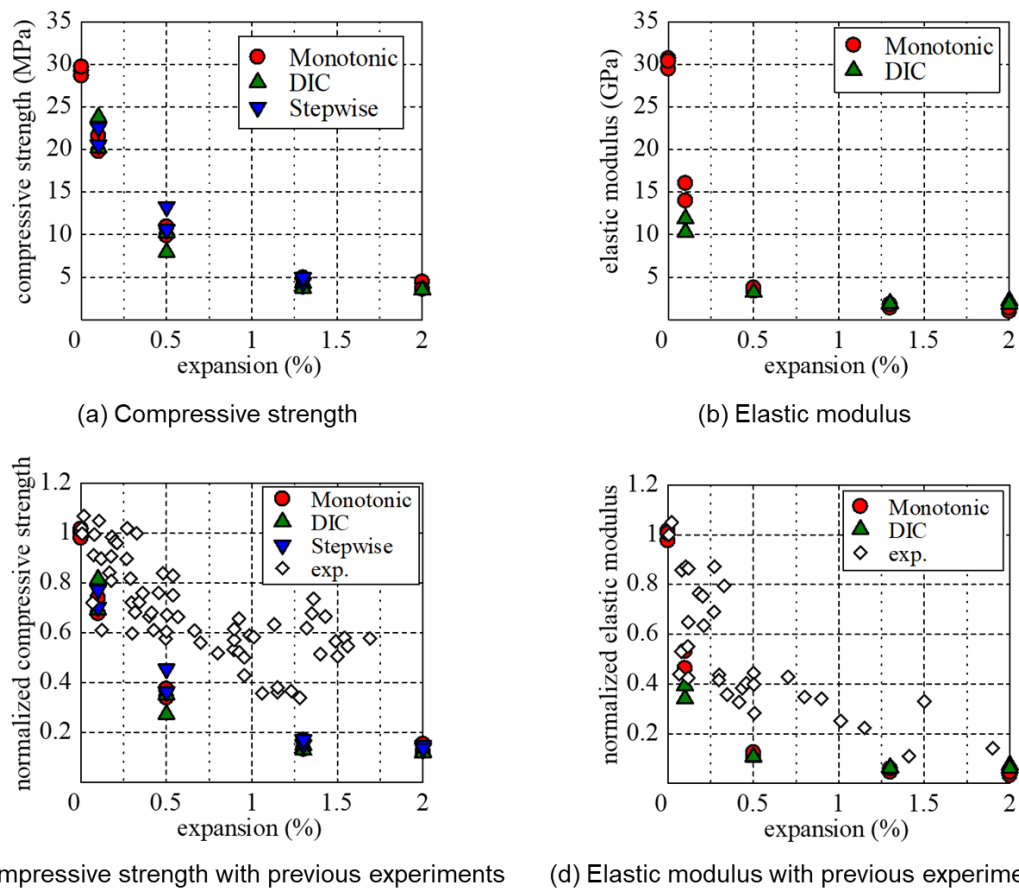


Figure 3.2: Changes in compressive behaviors

### 3.3 DIC

The distributions of tensile and compressive principal strains obtained by DIC are shown in Figure 3.3. The strain distributions were measured after the specimen attained 0.1, 0.5, 1.3, and 2.0 % expansion at the 20% stress level, which generally belongs to the elastic zone of normal concrete. The strain distribution results indicate that the compressive principal strains were generated at the interface of coarse aggregate particles in the compressive direction from the initial expansion of 0.1 %. From the 0.5 % expansion onward, further compressive principal strain accumulated at the interface of the large majority of aggregate particles, accompanied by strain generation in the mortar. This indicates the propagation of cracks into the mortar. The tensile principal strains were generated perpendicular to the loading direction, which resulted in vertical cracking as can be seen in Figure 3.3.

These principal strain distributions indicate the formation of debonding cracks at the interface of coarse aggregate particles and cracks in the mortar due to DEF-induced expansion. In addition, these cracks strongly affected the mechanical properties even from a low stress level. The debonding cracks at the interface of coarse aggregate particles caused significant reduction in the elastic modulus from the low expansion level because the compressive stress could not be easily transmitted to the aggregate particles and the stress-bearing effect of aggregate is thus reduced. In addition, as the expansion increased, debonding cracks occurred at the interface of the large majority of the aggregate particles, which further reduced the elastic modulus. In case of expansion beyond 0.5%, reduction in the elastic modulus did not change. This experimental evidence supports that the lower contribution of the stress-bearing effect of aggregates due to the generation of debonding cracks at the interface of aggregate particles causes large reduction in the elastic modulus.

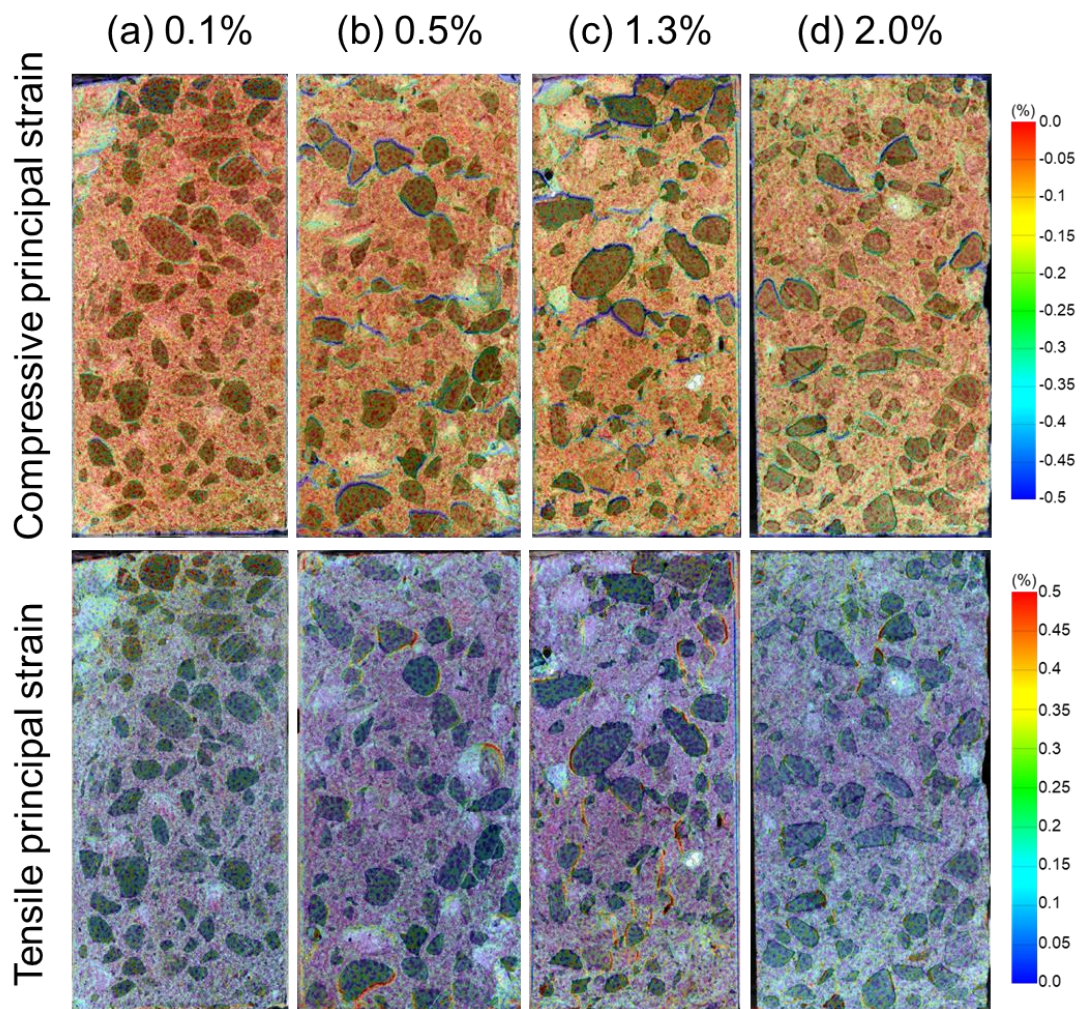


Figure 3.3: Strain distributions at a stress level of 20%

### 3.4 Stress–strain relationships

The stress–strain relationships of monotonic and stepwise cyclic loading are shown in Figure 3.4. In terms of monotonic loading, the strain at the compressive strength gradually increased with increasing expansion. The resulting strain at the compressive strength for 2.0% expansion was 7500 microstrains, which is four times that of the control specimens. In terms of stepwise cyclic loading, the plastic strain generated in each cyclic loading gradually increased with expansion. These plastic strains were generated from a low stress level and were significantly large even when the stress level is in the elastic zone. Furthermore, at the 50% stress level, the plastic strain increased with expansion, in particular, the plastic strain at 2.0% expansion reached 600 microstrains. Although such a significantly large plastic strain was generated during cyclic loading, the compressive strength and softening gradient were not different from those in the case of monotonic loading. This can be seen in Figure 3.2, which shows that the compressive properties did not change with the loading patterns. Therefore, it can be concluded that the plastic strain in the pre-peak stage generated during the cyclic loading does not affect the mechanical properties even if the plastic strain is significantly large. This indicates that the mechanical response of the plastic zone including the expansion-induced cracks under compressive stress is independent of the mechanical properties such as the compressive strength and softening gradient.

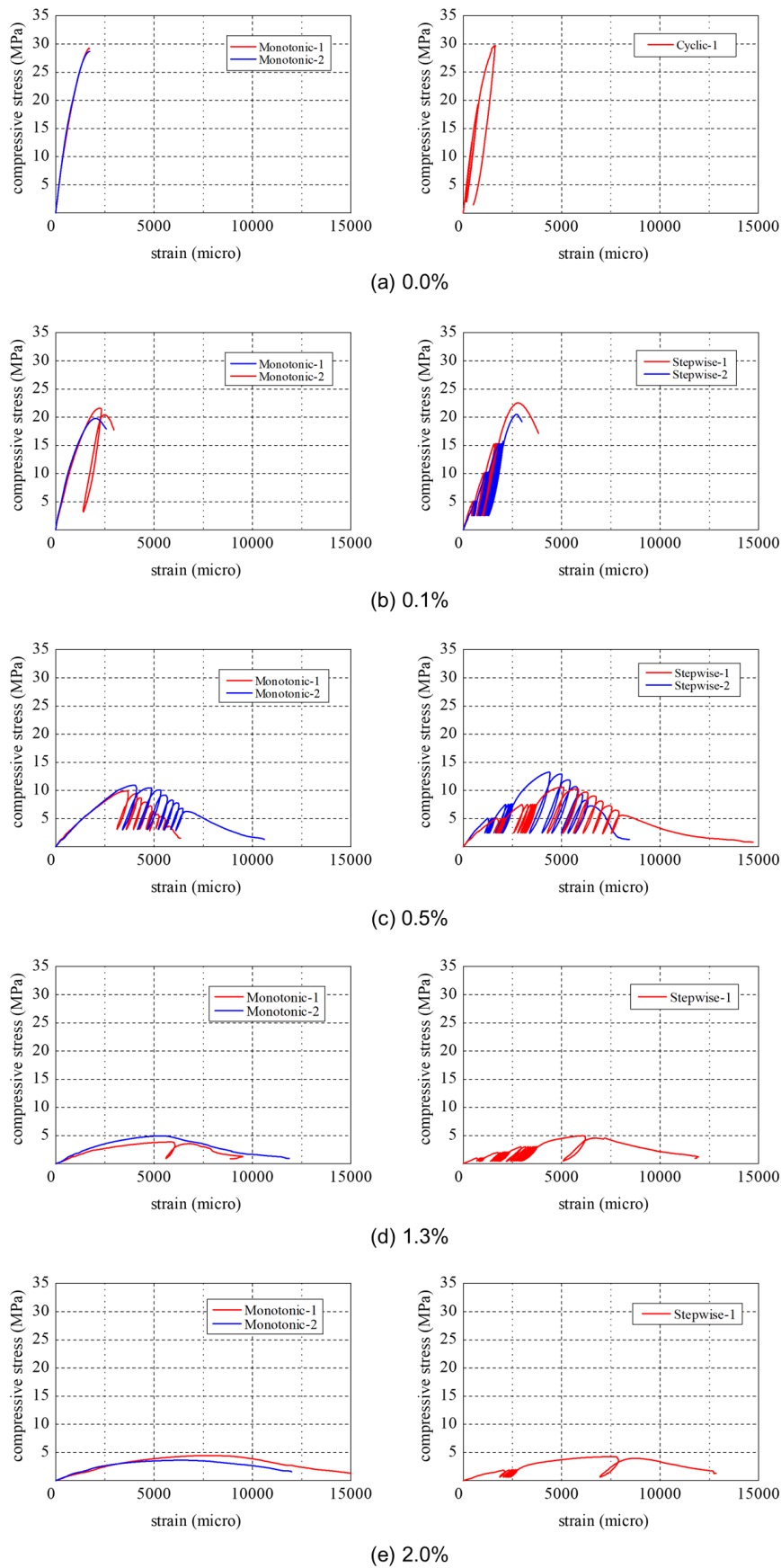


Figure 3.4: Stress–strain relationships

## 4. DISCUSSION

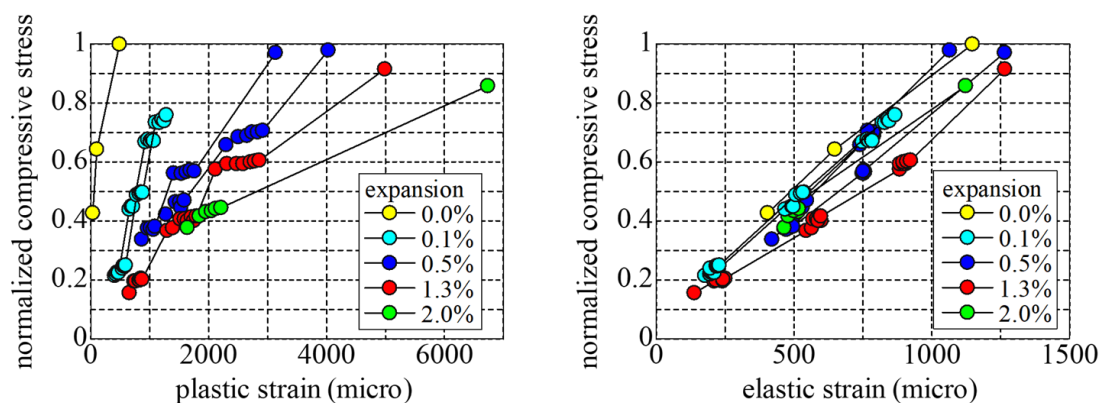
The compression tests indicated that the mechanical properties significantly reduced with an increase in the expansion. The tensile and compressive principal strain distributions obtained by DIC indicated the existence of debonding cracks at the paste-aggregate interfaces and cracks in the mortar due to DEF-induced expansion. The internal cracks strongly affect the reduction in mechanical properties even at a small expansion level. Furthermore, in stepwise cyclic loading, although significantly large plastic strains were generated during cyclic loading, the mechanical response of the plastic zone including expansion cracks under compressive stress was independent of the change in mechanical properties such as compressive strength and softening increment. In this section, we discuss the mechanical response of the plastic zone including internal cracks with the development of the elastic and plastic strains during stepwise cyclic loading.

The relationships between the elastic and plastic strains obtained from the stepwise cyclic loading and normalized compressive stress are shown in Figure 4.1. The plastic strains significantly increased with the expansion, while the elastic strains were independent of the expansion and reached 1000–1300 microstrains at the compressive strength in all expansion level cases. In addition, the increment gradient of elastic strain is also independent of the DEF-induced expansion. These unique trends of elastic strain are important information to understand the effect of DEF-induced expansion on mechanical properties.

In cyclic loading at a certain stress level, the plastic strains significantly increased while the elastic strains slightly increased. In this process, the strain distribution captured by DIC indicated the compression of internal cracks (Figure 3.3). To explain the unique evolution of plastic and elastic strains and DIC results, the schematic model of the stress-bearing network during compressive loading was illustrated in Figure 4.2. Note that it is assumed that the debonding cracks form at the interface of all the aggregate particles indicated in Figure 4.2 (a).

When the DEF-affected concrete is subjected to compression, the debonding cracks around the aggregate particles are likely to close until the crack faces come in contact with the others (Figure 4.2 (b) and (c)). This is evident from Figure 3.3. After contacting debonding cracks, a new stress transfer mechanism develops due to the stress-bearing of contacted crack faces, see Figure 4.2 (d).

The point of this model is whether the crack-closing process in the ITZ involves crack propagation, which has not been elucidated in previous studies. If the elastic zones resist the external force without any crack propagation during the crack-closing in the ITZ (Figure 4.2 (b)), it means that the area of the elastic zones is almost constant. On the contrary, it can be another assumption that crack propagation is involved in this process (Figure 4.2 (c)). In this case, the area of the elastic zones reduces due to crack propagation, leading to higher compressive stress acting on elastic zones at a given load. In the latter model, the elastic strains at a certain stress level should be increased based on Figure 4.2 (c), which is not consistent with the experimental evidence. The former model (Figure 4.2 (b)), on the contrary, can explain well why the compressive strength and softening increment of concrete for stepwise cyclic loading series were similar to those under monotonic loading despite significantly-large plastic strains in the pre-peak.



(a) Plastic strain development

(b) Elastic strain development

Figure 4.1: Plastic and elastic strain development from stepwise cyclic loading

The models shown in Figure 4.2 (b) and (d) are reasonable to account for the fact that the increment gradient of elastic strain indicates high linearity and that the elastic strain at compressive strength was independent of the expansion. Further investigation will be necessary to discuss the mechanical response of contacted crack faces with DEF expansion.

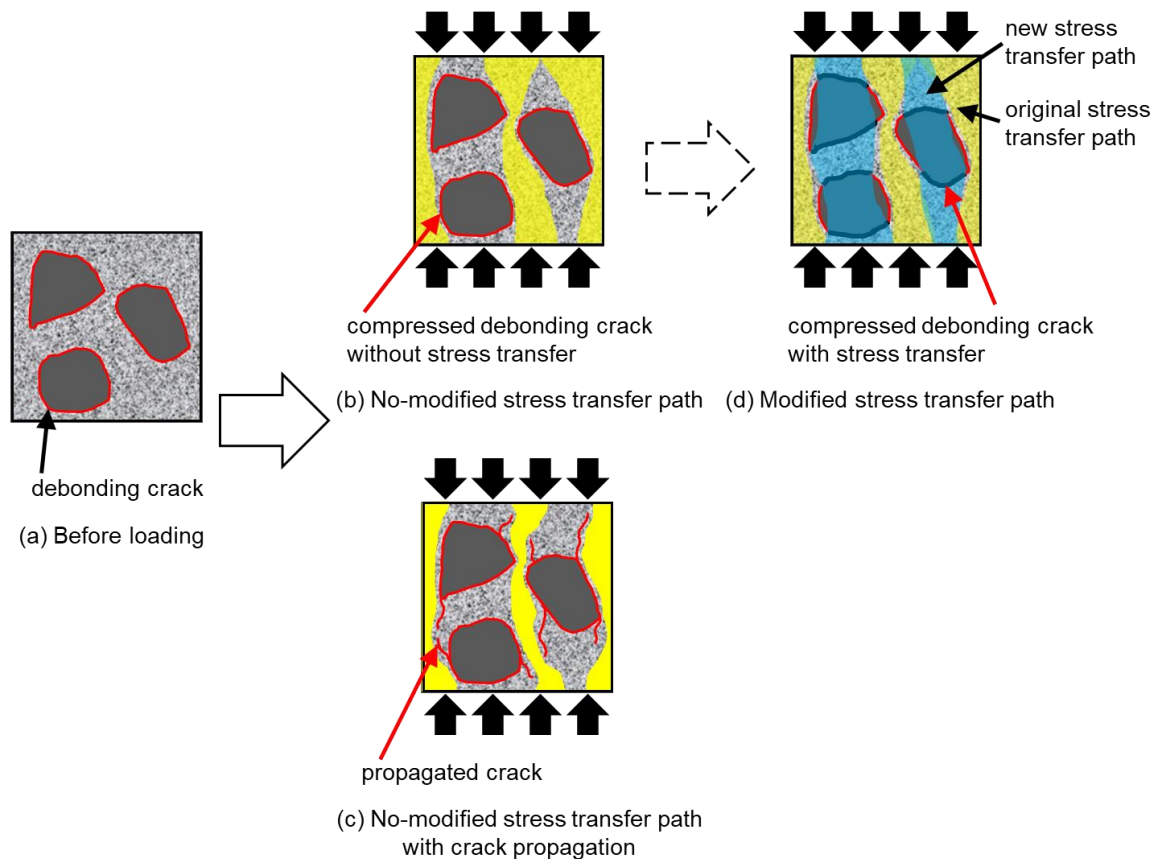


Figure 4.2: Concept of stress-bearing network during compressive loading

## 5. CONCLUSION

This study involved two types of uniaxial compressive loading (monotonic loading and stepwise cyclic loading) on cylindrical concrete specimens deteriorated by DEF under the stress-free condition. In monotonic loading, by visualizing the distributions of compressive and tensile principal strains by DIC, the mechanical response of expansion-induced cracks under compressive stress was evaluated. In stepwise cyclic loading, the mechanical response of internal cracks (debonding cracks at the paste-aggregate interfaces and cracks in the mortar) due to DEF-induced expansion was discussed from the perspective of the development of elastic and plastic strains. The main findings of this study can be summarized as below.

- (1) At 2.0 % expansion, the compressive strength decreased down to a ratio of 13.3 % and the elastic modulus decreased down to a ratio of 5.4 %. The loading types did not affect the compressive property changes.
- (2) The compressive and tensile principal strains were generated from a low stress level. At the initial stage of expansion of 0.1 %, debonding cracks generated at the interfaces of aggregate particles. In addition, for an expansion of 0.5 % and more, cracks in the mortar were observed. These cracks may cause the reduction in the mechanical properties from a low stress level.

- (3) The stress–strain relationships indicated that the compressive strength and the softening gradient for stepwise cyclic loading were not different from those of monotonic loading in spite of the generation of a larger plastic strain in the pre-peak stage.
- (4) In stepwise cyclic loading, both the increment gradient of elastic strain and the elastic strain at the peak strength did not change due to expansion, while the plastic strain increased with expansion. Furthermore, the strain development during cyclic loading at a certain stress level indicated that the internal cracks formed due to DEF-induced expansion were solely compressed without any crack propagation, which explains the experimental evidence that the compressive strength and the post-peak behavior did not differ from those under monotonic loading although significantly large plastic strains were generated in the pre-peak stage under stepwise cyclic loading.

## References

- [1] Diamond S (1996) Delayed Ettringite Formation – Processes and Problems. *Cem. Concr. Res.* 18:205-215.
- [2] Taylor HFW, Famy C, Scrivener KL (2001) Delayed Ettringite Formation. *Cem. Concr. Res.* 31:683-693.
- [3] Brunetaud X, Divet L, Damidot D (2008) Impact of unrestrained Delayed Ettringite Formation-induced expansion on concrete mechanical properties. *Cem. Concr. Res.* 38:1343-1348.
- [4] Bouzabata H, Multon S, Sellier A, Houari H (2012) Effects of restraint on expansion due to delayed ettringite formation. *Cem. Concr. Res.* 42:1024-1031.  
<https://doi.org/10.1016/j.cemconres.2012.04.001>
- [5] Martin RP, Sanchez L, Fournier B, Toulemonde F (2017) Evaluation of different techniques for the diagnosis & prognosis of Internal Swelling Reaction (ISR) mechanisms in concrete. *Constr. Build. Mater.* 156:956-964. <https://doi.org/10.1016/j.conbuildmat.2017.09.047>
- [6] Giannini ER, Sanchez LFM, Tuinukuafe A, Folliard KJ (2018) Characterization of concrete affected by delayed ettringite formation using the stiffness damage test. *Constr. Build. Mater.* 162:253-264. <https://doi.org/10.1016/j.conbuildmat.2017.12.012>
- [7] Multon S, Toulemonde F (2006) Effect of applied stresses on alkali–silica reaction-induced expansions. *Cem. Concr. Res.* 36:912-920.
- [8] Gautam BP, Panesar DK, Sheikh SA, Vecchio FJ (2017) Multiaxial expansion-stress relationship for alkali silica reaction-affected concrete, *ACI Materials Journal* 114-M17:171-184.
- [9] Dunant CF, Scrivener KL (2012) Effects of uniaxial stress on alkali-silica reaction induced expansion of concrete. *Cem. Concr. Res.* 42:567-576.  
<https://doi.org/10.1016/j.cemconres.2011.12.004>
- [10] Kawabata Y, Ueda N, Miura T, Multon S (2021) The influence of restraint on the expansion of concrete due to delayed ettringite formation. *Cem. Concr. Comp.* 121.  
<https://doi.org/10.1016/j.cemconcomp.2021.104062>
- [11] Hansen SG, Hoang LC (2021) Anisotropic compressive behavior of concrete from slabs damaged by alkali-silica reaction. *Constr. Build. Mater.* 267.  
<https://doi.org/10.1016/j.conbuildmat.2020.120377>
- [12] Sanchez LFM, Drimalas T, Fournier B, Mitchell D, Bastien J (2018) Comprehensive damage assessment in concrete affected by different internal swelling reaction (ISR) mechanisms. *Cem. Concr. Res.* 107:284-303. <https://doi.org/10.1016/j.cemconres.2018.02.017>
- [13] Ahmed T, Burley E, Rigden S, Abu-Tair AI (2003) The effect of alkali reactivity on the mechanical properties of concrete. *Constr. Build. Mater.* 17:123-144.
- [14] Giaccio G, Zerbino R, Ponce JM, Batic OR (2008) Mechanical behavior of concretes damaged by alkali-silica reaction. *Cem. Concr. Res.* 38:993-1004.
- [15] Gautam BP, Panesar DK, Sheikh SA, Vecchio FJ (2017) Effect of coarse aggregate grading on the ASR expansion and damage of concrete. *Cem. Concr. Res.* 95:75-83.

- [16] Sanchez LFM., Fournier B, Jolin M, Mitchell D, Bastien J (2017) Overall assessment of Alkali-Aggregate Reaction (AAR) in concretes presenting different strengths and incorporating a wide range of reactive aggregate types and natures. *Cem. Concr. Res.* 93:17-31.
- [17] Giannini ER (2012) Evaluation of concrete structures affected by alkali-silica reaction and delayed ettringite formation, Doctoral Thesis, The University of Texas at Austin.
- [18] Miura T, Sato K, Fujishima M, Nakamura H, Kawabata Y (2022) Mechanism for reduction in compressive properties of cementitious materials in relation to internal crack patterns due to ASR and DEF expansion. *Cem. Concr. Comp.* 128.
- [19] Onoue K. Matsushita H (2012) Reduction mechanism of fatigue strength of concrete under compression due to permeation of liquids. *Constr. Build. Mater.* 37:82-92.